In Proceedings of the 9th International Symposium on Unsteady Aerodynamics, Aeroacoustics and Aeroelasticity of Turbomachines (ISUAAAT) and Legendre Lecture Series, Lyon, France, Sept. 4-8, 2000. Edited by Pascal Ferrand and Stephane Aubert, pp. 750-761. Presses Universitaires de Grenoble.

COMPUTATION OF CASCADE FLUTTER WITH A COUPLED AERODYNAMIC AND STRUCTURAL MODEL

M. SADEGHI AND F. LIU
Department of Mechanical and Aerospace Engineering
University of California, Irvine, CA 92697-3975, USA

Abstract. A computational method for flutter simulation of turbomachinery cascades is presented. The flow through multiple blade passages is calculated using a time-domain approach with coupled aerodynamic and structural models. The unsteady Euler/Navier-Stokes equations are solved in 2D using a second-order implicit scheme with dual time-stepping and a multigrid method. A structural model for the blades is integrated in time together with the flow field. Information between structural and aerodynamic models is exchanged until convergence in each real-time step. The computations are performed on parallel computers using the Message Passing Interface (MPI). Computational results for a cascade are presented and compared with those obtained by the conventional energy method and with experimental and numerical data by other authors. Significant differences are found between the two methods at low mass ratios. Possibilities of nonlinear flutter are demonstrated at certain transonic conditions.

1. Introduction

Flutter calculations for turbomachinery blade rows often employ Lane's traveling wave model [1], in which the adjacent blades in a blade row are assumed to vibrate at the same frequency but with a constant phase difference, the Inter-Blade Phase Angle (IBPA). With this model, aerodynamic responses of the blade row can be determined by using a single blade passage with a phase-shifted periodic boundary condition. The use of the phase-shifted boundary condition and its implementation in a flow code implies that the solution is both temporally and spatially periodic. This is not true in a general case, unless the oscillation is neutrally stable. In general, the interaction between aerodynamic forcing and structural behavior leads

to an increasing oscillation amplitude, when flutter happens. The IBPA does not necessarily stay constant, either, and there may be an interaction between different torsional and bending oscillation modes. In the simplest linear case, however, all but one mode and IBPA will eventually disappear. Only the most critical mode will survive.

Flutter investigation with the uncoupled approach is done by specifying the mode of the blade oscillation and the IBPA and then using the energy method to determine whether the specified oscillation leads to stabilizing or destabilizing aerodynamic forces. The oscillation frequency is usually assumed to be equal to the eigenfrequency of the blade at the investigated mode, on the assumption that the blades are relatively stiff and the blade inertia is large. These assumptions are not necessary in a time marching approach with coupled aerodynamics and structure dynamics. The most critical mode will automatically dominate the solution, since stable modes die out. The coupled calculation is more expensive than a single run with the uncoupled approach, but the latter needs many runs with different IBPAs and modes to find the most unstable case. In total, the coupled approach may require less computational time.

An investigation of stall flutter in linear cascade was done by Sisto et al. [2], [3]. The authors used a vortex and boundary layer method for incompressible flow coupled with a spring model for the blade motion. A similar torsional spring and linear spring model for rigid profiles was used by Bakhle et al. [4], by Hwang and Fang [5], and by Alonso and Jameson [6]. Bakhle et al. investigated potential flow through a cascade. A case with linear flow behavior was chosen in order to validate the coupled method by comparison with uncoupled results. Hwang et al. solved the Euler and Navier-Stokes equations through a cascade on unstructured grids. Alonso and Jameson developed a parallel method for flutter simulation of isolated wings.

A major advantage of the coupled method over the uncoupled approach is the ability to capture phenomena that are nonlinear in time. Recently, Carstens and Belz [7] performed numerical investigations on a compressor cascade with the blades oscillating in a torsional mode. Significant nonlinear effects were discovered with this cascade at transonic flow conditions. The cascade was found to develop a flow pattern with choked flow and an oscillating shock in each odd numbered passage, and purely subsonic flow in each even numbered passage.

In a previous work by Ji and Liu [8] a Navier-Stokes code with a two-equation k-ω turbulence model by Wilcox [9] was developed to calculate quasi-three-dimensional unsteady flows around multiple oscillating turbine blades. The pseudo-time approach by Jameson [10] is used in conjunction with a time-accurate multigrid method. The code was made parallel by us-

ing the Message Passing Interface MPI so that multiple passages could be calculated without the use of phase-shifted periodic boundary conditions for blade flutter problems. Therefore, the blade motion does not have to be periodic, neither spatially nor temporally. The code was used to perform uncoupled studies in [11] and is here extended to perform coupled calculations by including a structural model. The aerodynamic and structural equations are solved simultaneously in each real-time step. The elastic behavior of a blade is modeled with a linear spring for the bending motion and a torsional spring for the rotational degree of freedom. Euler calculations are performed and compared with experimental results by Buffum and Fleeter [12], for a cascade of biconvex airfoils. Differences between the uncoupled method and the coupled method are demonstrated for that test case. An unstaggered cascade of NACA profiles, at pure torsion as well as at coupled torsion and bending, is used to study the nonlinear phenomenon discovered by Carstens and Belz [7].

2. Coupled flow and structure solver

A quasi-three-dimensional finite volume method is used to calculate the flow through a cascade. Details of the method are given in [8]. A second order accurate scheme is used for spatial discretization. In semi-discrete form, the unsteady conservation equations for mass, momentum and energy can be written as

$$\frac{d\mathbf{w}}{dt} + \mathbf{R}(\mathbf{w}) = 0 \tag{1}$$

where the vector $\mathbf{w} = [\rho,\ \rho u,\ \rho v,\ \rho E,\ \rho k,\ \rho\omega]^T$ contains the conservative flow variables plus the turbulent kinetic energy k and the specific dissipation rate ω, in the k-ω turbulence model by Wilcox [9]. The vector of residuals $\mathbf{R}$ consists of the spatially discretized flux balances. Time accuracy is achieved by using a second order implicit time-discretization scheme which is recast into a pseudo-time formulation, as proposed by Jameson [10]:

$$\frac{d\mathbf{w}^{n+1}}{dt^*} + \mathbf{R}^*(\mathbf{w}^{n+1}) = 0 \tag{2}$$

with

$$\mathbf{R}^*(\mathbf{w}^{n+1}) = \frac{3\mathbf{w}^{n+1} - 4\mathbf{w}^n + \mathbf{w}^{n-1}}{2\Delta t} + \mathbf{R}(\mathbf{w}^{n+1}) \tag{3}$$

where t^* is a pseudo-time, Δt is the time step size in real-time, $\mathbf{w}^{n-1}$ and $\mathbf{w}^n$ are the flow solutions at the two previous real-time levels. The steady state solution of Eq. (2) in the pseudo-time t^* is equivalent to the time accurate solution of Eq. (1) at the time level t^{n+1} with a second order implicit scheme, $\mathbf{R}^*(\mathbf{w}^{n+1}) = 0$. Equation (2) is then solved efficiently by a

conventional Runge-Kutta type scheme with multigrid, local time stepping, and residual smoothing [8]. The flow in each blade passage of the cascade is calculated on its own processor. The Message Passing Interface (MPI) is used to exchange boundary information between adjacent blade passages. More detailed information regarding the parallel implementation can be found in [8].

In general, a finite-element model for a structural system leads to the following equation

$$[M]\ddot{\mathbf{q}} + [K]\mathbf{q} = \mathbf{F} \tag{4}$$

where $[M]$ is the mass matrix, $[K]$ is the stiffness matrix and $\mathbf{F}$ is the forcing vector. A modal approach is used to solve Eq. (4). Considering a finite number of N eigenmodes, Eq. (4) can be transformed into N decoupled modal equations

$$\ddot{\eta}_i + 2\zeta_i\omega_i\dot{\eta}_i + \omega_i^2\eta_i = Q_i, \quad i = 1, N \tag{5}$$

where η_i are the generalized coordinates in direction of the normalized eigenvectors $\boldsymbol{\phi}_i$, such that $Q_i = \boldsymbol{\phi}_i^T\mathbf{F}$, $\omega_i^2 = \boldsymbol{\phi}_i^T[K]\boldsymbol{\phi}_i$, $\boldsymbol{\phi}_i^T[M]\boldsymbol{\phi}_i = 1$, and ζ_i is the modal damping of the i-th mode that has been introduced to the model.

Following Alonso and Jameson [6], Eq. (5) is transformed into a system of two first-order differential equations and then discretized and recast into a pseudo-time problem in the same form as Eqs. (2) and (3) for the flow equations. Thus we have

$$\frac{d\mathbf{z}^{n+1}}{dt^*} + \mathbf{R}_s^*(\mathbf{z}^{n+1}) = 0 \tag{6}$$

and

$$\mathbf{R}_s^*(\mathbf{z}^{n+1}) = \frac{3\mathbf{z}^{n+1} - 4\mathbf{z}^n + \mathbf{z}^{n-1}}{2\Delta t} + \mathbf{R}_s(\mathbf{z}^{n+1}) \tag{7}$$

where $\mathbf{z}$ is the vector of displacements and displacement velocities. Notice that the aeroelastic Eqs. (6) and (7) are coupled with the flow Eqs. (2) and (3) since the residual $\mathbf{R}(\mathbf{w})$ depends implicitly on $\mathbf{z}$ through the flow boundary conditions and the residual $\mathbf{R}_s(\mathbf{z})$ depends on $\mathbf{w}$ through the aerodynamic forcing. Equations (2) and (6) form a coupled system in pseudo-time which can be solved by the same explicit Runge-Kutta scheme. In principle, Eqs. (2) and (6) can be marched in pseudo-time simultaneously, i.e. when Eq. (2) is marched one pseudo-time step, Eq. (6) is also marched by one pseudo-time step. In practice, it is found that this procedure may lead to divergence because the flow equations usually converge slower in pseudo-time than the structural equations. Intermediate flow solutions may lead

to inaccurate aerodynamic forcing, which in turn would cause a large deformation in the structures, resulting in potential divergence. In view of the above, the flow equations are marched 10 pseudo-time steps before the structural equations are also marched 10 pseudo-time steps, followed by an update of the grid coordinates, grid velocities and the blade forces. In this way, both iterations, for the flow model and the structural model, are converging in a coupled manner within each real-time step.

3. Results and Discussion

Previous investigations were done, using the uncoupled method, [8], [11]. In the current work, we are presenting comparisons between the uncoupled method and the coupled method. An experimental test case by Buffum and Fleeter [12] was chosen for this purpose. A linear cascade of uncambered biconvex airfoils was tested for several inter-blade phase angles and two different reduced oscillation frequencies. The airfoils, with a thickness-to-chord ratio of 7.6% and with a stagger angle of 53^o, were oscillated in a pure rotational mode around mid-chord, with an amplitude of 1.2^o, an inlet Mach number of 0.65 and an incidence angle of 0^o. Buffum and Fleeter performed measurements with either all blades oscillating, or with only one oscillating blade and using the method of influence coefficients. They compared the experimental data with results from linearized theory for a flat plate. Details of the configuration are published in [12]. We first perform Euler calculations with the uncoupled method, i.e. the blades are forced to vibrate at prescribed torsional motions with given frequencies and IBPAs.

3.1. UNCOUPLED CALCULATIONS

Figures 1 and 2 show the magnitude and phase of the unsteady pressure difference between upper and lower surface for the reduced frequency of $k = 0.223$. Figure 3 shows the work coefficient calculated for various IBPAs at $k = 0.223$. A positive work coefficient indicates an unstable condition. The agreement of the Euler results with the data provided in [12] is reasonably good for both inter-blade phase angles of 0^o, and 90^o. It appears that the Euler solutions are closer to those for the flat plate than to the experimental results, especially when comparing the work coefficient in Fig. 3.

3.2. FLUID-STRUCTURE COUPLED CALCULATION

In the uncoupled approach, the interaction between aerodynamics and structure is neglected. The blades are externally forced to oscillate with a specified constant amplitude and inter-blade phase angle. The work done on the blade by aerodynamic forces, as shown in Figure 3, is an indicator

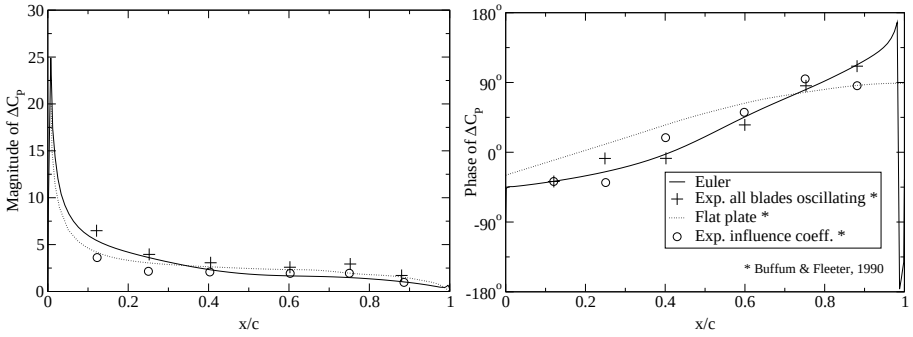

Figure 1. Unsteady pressure difference coefficient, $IBPA = 0^o$, $k = 0.223$

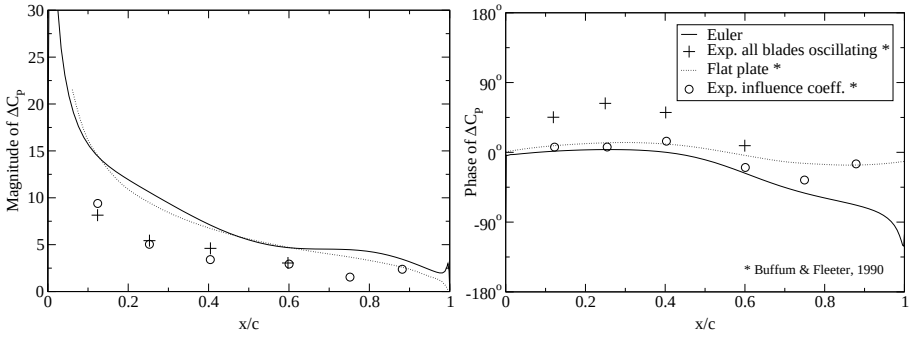

Figure 2. Unsteady pressure difference coefficient, $IBPA = 90^o$, $k = 0.223$

for stability. Positive work indicates that the aerodynamic moment amplifies the oscillation, in the case of negative work the moment stabilizes the motion. However, this is only true when the blades are oscillating in the prescribed motion. In an actual system, the blades are driven by the aerodynamic forces. Therefore, the motion of the blade will generally not follow a prescribed pattern with constant amplitude and IBPA. The motion will depend on the mass ratio of the blades as well as the flow conditions. The frequency of the oscillation will also be shifted from the structural eigenfrequency of the system.

In this section we use an airfoil model with two degrees of freedom, similar to the model used by [4], [5] and [6]. This is represented by the following mass and stiffness matrices, forcing vector and displacement vector in Eq. (4).

$$[M] = \begin{bmatrix} 1 & x_\alpha \\ x_\alpha & r_\alpha^2 \end{bmatrix}, \qquad [K] = \begin{bmatrix} (\frac{\omega_h}{\omega_\alpha})^2 & 0 \\ 0 & r_\alpha^2 \end{bmatrix}$$

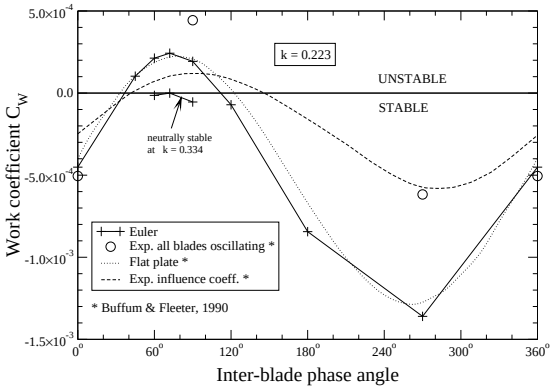

Figure 3. Work coefficient, $k = 0.223$

$$\mathbf{F} = \frac{1}{\pi\mu k_\alpha^2} \begin{Bmatrix} -C_l \\ 2C_m \end{Bmatrix}, \qquad \mathbf{q} = \begin{Bmatrix} \frac{h}{b} \\ \alpha \end{Bmatrix}$$

Here, ω_h and ω_α are the eigenfrequencies of the uncoupled translational and rotational degrees of freedom, corresponding to the translational displacement h/b and the rotational displacement α. The distance between the center of rotation and the center of gravity x_α, and the radius of gyration r_α are non-dimensionalized with the semi-chord b, C_l and C_m are the coefficients of lift and moment, $k_\alpha = \omega_\alpha b/u_\infty$ is the reduced rotational eigenfrequency and $\mu = m/\rho_\infty \pi b^2$ the mass ratio, where the index ∞ denotes undisturbed inlet properties.

In the case of a single degree of freedom with pure torsion, the structural behavior is determined by specifying two parameters, here the torsional eigenfrequency ω_α and the mass ratio μ of the blade:

$$\omega_\alpha = \sqrt{\frac{K_\alpha}{I_\alpha}} \qquad \mu = \frac{m}{\pi\rho_\infty b^2}$$

where K_α and I_α are the spring constant and moment of inertia, m is the blade mass per unit span, ρ_∞ is the undisturbed density and b the half chord length.

For a mass ratio of $\mu = 450$, Fig. 4 shows the total energy of all blades in the cascade over time at three different reduced eigenfrequencies, obtained with the coupled approach. One of the solutions is unstable with positive work increasing the total energy of the blades, one is neutrally stable with effectively no work done, and the highest frequency leads to a stable solution, where negative work decreases the blade energy. These calculations where performed with five blade passages, allowing for an inter-blade phase

angle of 72^o and its multiples, which was recognized as the most unstable $IBPA$ in Fig. 3.

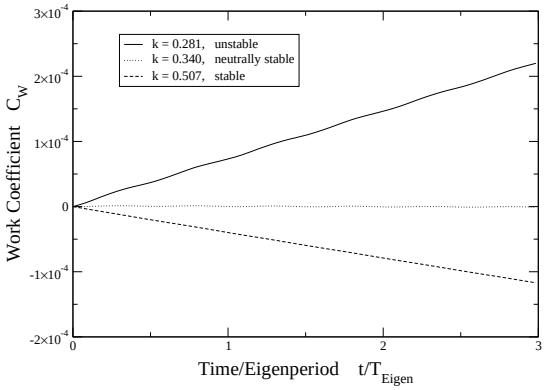

Figure 4. Total energy of the cascade over time at $\mu = 450$

The mass ratio determines how much the aerodynamic forcing influences the blade motion. With a very large mass ratio, the aerodynamic forces have little effect on the eigenfrequency and eigenmode of the system. In this case of a single degree of freedom, the oscillation is purely harmonic at the reduced eigenfrequency k and with a constant amplitude. Therefore, the coupled solution with very high mass ratio is expected to be close to the solution of the uncoupled method. However, as the mass ratio decreases, the solution of the coupled method will be different from the uncoupled result, and the actual oscillation frequency will vary from the eigenfrequency of the blade.

Figure 5 shows the reduced eigenfrequency and oscillation frequency at which the blade motion is neutrally stable, as a function of the mass ratio. In order to find the neutral frequency for a given mass ratio, the eigenfrequency is chosen by *trial and error* until the total energy is found to be constant in time, as done for $\mu = 450$ in Fig. 4. The actual blade oscillation frequency is then recorded as the actual neutral oscillation frequency shown in Fig. 5. Notice that for this case with only one oscillation mode in one degree of freedom, the actual oscillation frequency at which the motion is neutral does not depend on the structural parameters, but is unique. It is not significant how the blade is caused to oscillate at that unique neutral frequency, it can be either artificially forced by the uncoupled method, or resulting from aerodynamic-structural interaction. There is only one solution for which the aerodynamic forces do effectively no work on the blades. Figure 5 verifies that the lower the mass ratio, the larger the difference between the eigenfrequency and the actual oscillation frequency.

The uncoupled method yields the neutral *oscillation frequency* since it is based on assuming an actual oscillation frequency in the calculation. However, it gives no information on the *eigenfrequency* for which the blades will oscillate at that neutral frequency. Only if the mass ratio is large enough, those two frequencies are similar and the uncoupled approach is useful. At low mass ratios, e.g. with a blade that is hollow to allow for cooling, the assumption that the blades will oscillate at their eigenfrequencies would lead to significant errors.

For this test case, the blades oscillate at a frequency lower than the eigenfrequency. A system with an eigenfrequency that is in the shaded region of Fig. 5 would be erroneously claimed to be stable by a decoupled method while the coupled method correctly predicts it to be unstable. With the biconvex profile used in this study, realistic mass ratios for a solid blade are between $\mu_{Ti} = 250$ for titanium and $\mu_{St} = 450$ for steel (based on standard atmospheric density). In this range the difference between eigenfrequency and oscillation frequency may be up to 5%, as seen in Fig. 5.

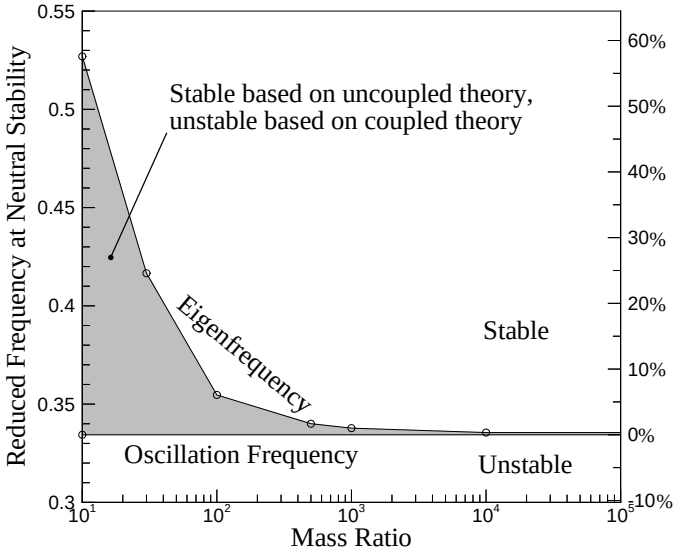

Figure 5. Frequency at neutral stability over mass ratio

3.3. NONLINEAR FLUTTER

Carstens and Belz also developed a computer code for simulating flutter in the time domain [7]. They discovered some nonlinear phenomena in a

two-dimensional cascade with a torsional degree of freedom. Similar nonlinear behaviors are found in this paper for a similar cascade at transonic conditions. This is a cascade with unstaggered NACA0006 profiles, a gap-to-chord ratio of 1.0, a torsional axis position at $x_a = 38\%$ chord, $y_a = 0$, and a mass ratio of $\mu = 192$ (solid titanium blade). Hwang and Fang [5] investigated this cascade but reported no nonlinear effects at the conditions they studied. In this paper an inlet Mach number of 0.65 is chosen such that the steady state solution is purely subsonic, but when oscillating, the flow in some blade passages becomes partially supersonic and chokes. The inlet flow angle is zero degrees. The coupled approach is applied for two cases: oscillation in pure torsion, and with coupled torsion and bending. In the latter case, the torsional and bending eigenfrequencies are chosen to be equal ($k_\alpha = k_h = k$).

Calculations with two blade passages at various eigenfrequencies k revealed, that this test case does not behave as linearly as the biconvex profile cascade described in the previous sections. Figure 6 shows the time history of the angular deflections of both blades, with only the torsional degree of freedom. The blades are initially forced to move a few periods at their eigenfrequency and are then set free to be governed by the aerodynamics. At eigenfrequencies below $k = 0.049$ the blade motion is unstable (not shown in the figure), but when the frequency is increased, an interesting phenomenon appears. At a reduced frequency of $k = 0.049$ the initial oscillation still exhibits growth as for the lower frequencies. However, at some finite deflection, the blades start to branch apart and oscillate around two different mean conditions. Eventually they settle down at the two distinct mean conditions and become stable. The blade positions and the Mach number contours in the flow field are also shown in Fig. 6. It can be seen from this figure that one flow passage acts as a subsonic nozzle, the other one as a choked Laval nozzle.

When the eigenfrequency is increased to $k = 0.059$, the oscillation is neutrally stable around some final deflection smaller than the one at lower frequencies, Fig. 6. Interestingly, the deflections at $k = 0.059$ are symmetric, unlike the final deflections at $k = 0.049$. At higher eigenfrequencies ($k \geq 0.074$) the cascade is stable at zero deflection.

Figure 7 shows the angular and translational displacements for the same cascade with coupled torsional and bending degrees of freedom. The basic behavior is the same as for the case with torsional motion only. However, the condition of asymmetric deflection is not found for this case.

Unlike the compressor cascade studied by Carstens and Belz [7], the pattern with alternating choked and subsonic flow seems to be stable or at least neutrally stable for the cascade studied in this paper. The NACA cascade exhibits the above nonlinear phenomena throughout a range of

eigenfrequencies, but is found to be stable or neutrally stable under all studied conditions.

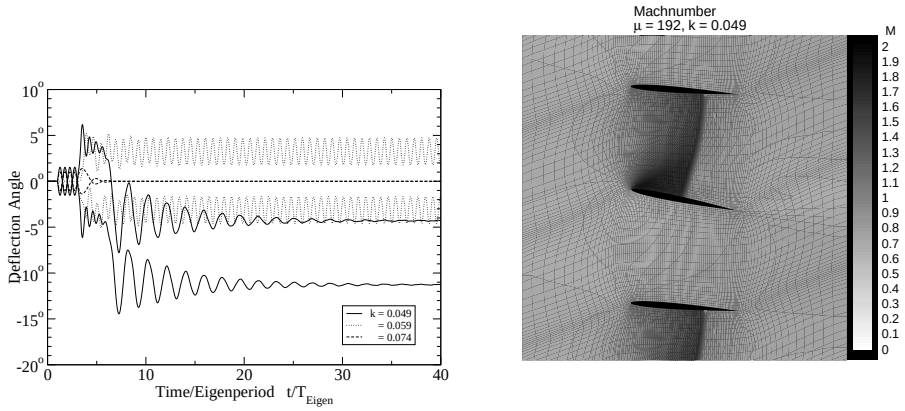

Figure 6. Pure torsion: rotational deflection over time, and Mach number distribution for $k = 0.049$

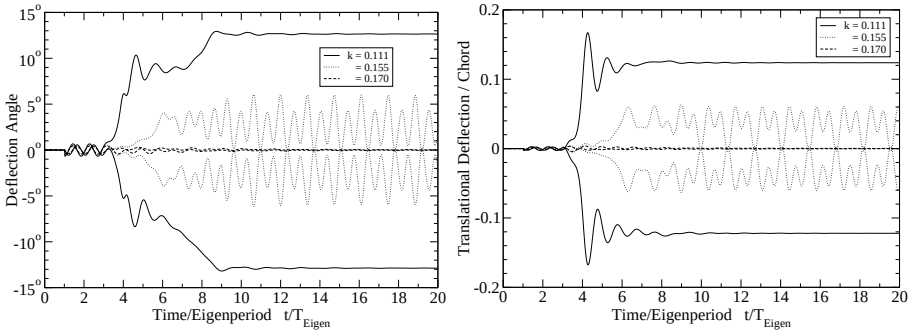

Figure 7. Bending + torsion: rotational and translational deflection over time

4. Conclusions

A coupled aerodynamics-structural dynamics method is presented. The quasi-3D Euler/Navier-Stokes equations and the structural modal equations for a two-DOF blade model are solved simultaneously in the time domain. For this presentation, only Euler calculations are performed. The conventional uncoupled (energy) method determines a stability boundary by assuming that the blades oscillate at their natural frequencies. Computations with the coupled method demonstrate significant differences between the natural frequencies of the blades and the actual flutter frequency at low

mass ratios. In the case of biconvex profiles with a single degree of freedom studied in this paper, the oscillation frequency is lower than the structural eigenfrequency. Therefore, if the mass ratio is low, the uncoupled method would predict stability, while the coupled method predicts instability.

Nonlinear flutter behaviors are demonstrated for a cascade with unstaggered NACA profiles at transonic conditions in either torsional motion or combined torsional and bending motion. Within a certain range of structural eigenfrequencies, initial instability may push the blades away from the initial mean blade positions so that they oscillate or settle down at different mean positions for different blades in the cascade. When this happens, one passage of the cascade is choked while its neighbor passage functions as a subsonic nozzle.

References

1. Lane, F. (1956) "System Mode Shapes in the Flutter of Compressor Blade Rows", *Journal of the Aeronautical Sciences*, pp. 54-66
2. Sisto, F., Thangam, S., and Abdel-Rahim, A. (1991) "Computational Prediction of Stall Flutter in Cascaded Airfoils", *AIAA Journal*,**Vol. 29**, pp. 1161-1167
3. Abdel-Rahim, A., Sisto, F., and Thangam, S. (1993) "Computational Study of Stall Flutter in Cascaded Airfoils", *Journal of Turbomachinery*,**Vol. 115**, pp. 157-166
4. Bakhle, M. A., Reddy, T. S. R., and Keith, T. G. Jr. (1992) "Time Domain Flutter Analysis of Cascades Using a Full-Potential Solver", *AIAA Journal*,**Vol. 30**, pp. 163-170
5. Hwang, C. J., and Fang, J. M. (1999) "Flutter Analysis of Cascades Using an Euler/Navier-Stokes Solution-Adaptive Approach", *Journal of Propulsion and Power*,**Vol. 15**, pp. 54-63
6. Alonso, J. J., and Jameson, A. (1994) "Fully-Implicit Time-Marching Aeroelastic Solutions", *AIAA Paper 94-056*
7. Carstens, V., and Belz, J. (2000) "Numerical Investigation of Nonlinear Fluid-Structure Interaction in Vibrating Compressor Blades", *ASME Paper 2000-GT-0381*
8. Ji, S. and Liu, F. (1999) "Flutter Computation of Turbomachinery Cascades Using a Parallel Unsteady Navier-Stokes Code", *AIAA Journal*,**Vol. 37**, pp 320-327
9. Wilcox, D. C. (1988) "Reassessment of the Scale-Determining Equation for Advanced Turbulence Models", *AIAA Journal*,**Vol. 26**, pp. 1299-1310
10. Jameson, A. (1991) "Time Dependent Calculations Using Multigrid, with Applications to Unsteady Flows Past Airfoils and Wings", *AIAA Paper 91-1596*
11. Sadeghi, M. and Liu, F. (2000) "A Method for Calculating Mistuning Effects on Cascade Flutter", *AIAA Paper 2000-0230*
12. Buffum, D. H., and Fleeter, S. (1990) "Oscillating Cascade Aerodynamics by an Experimental Influence Coefficient Technique", *Journal of Propulsion*,**Vol. 6**, pp 612-620